Magazine of Civil Engineering

ISSN 2712-8172

journal homepage: http://engstroy.spbstu.ru/

DOI: 10.18720/MCE.99.3

Numerical simulation of concrete dam during heavy rain

***G. Lei*[a,b,c], *S. Weiping*[a], *G. Lixia*[a,b,c*], *W. Lunyan*[a,b,c]**

[a] *School of Water Conservancy, North China University of Water Resources and Electric Power, Zhengzhou, China*

[b] *Henan Water Valley Research Institute, Zhengzhou, China*

[c] *Henan Key Laboratory of Water Environment Simulation and Treatment, Zhengzhou, China*

** E-mail: guolx@126.com*

Keywords: dams, finite element method, numerical simulaion, temperature, water level, stress analysis

Abstract. In recent years, the frequent extreme weather has led to the rise of reservoir water level, and accordingly changed the reservoir water temperature. As for concrete dams, changes in reservoir water temperature and air temperature may generate temperature stress, and such effect and sudden rise of water level will inevitably change the dam force and endanger the dam safety. By means of numerical simulation and theoretical analysis, this paper analyzed the effect of the extreme rainstorm on the reservoir water level and water temperature, and selected a typical project to simulate the changes of temperature field and stress field of concrete dams in an extreme rainstorm under different working conditions. Results showed that: (1) After the storm flood entered the reservoir, the temperature stress changed little due to the change in the reservoir water temperature; (2) During the rainstorm, the compressive and tensile stresses of concrete dams increased with the time, but did not exceed the allowable values of the concrete used for the dam body; therefore, the dam body was safe; (3) By comparing the effects of the reservoir water level rise caused by heavy rain on the dam stress, the dam temperature stress response varied with the water level rising rate: the greater the reservoir water level rising rate was, the greater the maximum dam response stress was. After being affected by the rainstorm, the dam stresses were the same. Therefore, it was necessary to use a dispatching method to control the rise of the water level. This study can provide theoretical basis and reference for the operation and dispatching of reservoirs during extreme rainstorms.

1. Introduction

As the global climate is worsening, the extreme weather frequently occurs in various regions, which has become a new trend [1]. Under this trend, heavy rains that are characterized by high intensity and short duration may cause floods that exceed the design limit of dams, posing severe challenges to the safe operation of dams and reservoir dispatching during the heavy rains [2–4].

For large and medium-sized reservoirs, due to the large catchment area and wide convergence area, the water level in the reservoirs will rise rapidly and the water temperature will change accordingly in case of a heavy rain. Short-duration, high-intensity heavy rain may cause the sudden rise of water level in reservoirs [5–8]. Zeng Kang et al. [9] found that the inflow conditions (water temperature, inflow rate) of reservoirs during the flood season would change significantly, and the rainfall runoff would reduce the vertical water temperature difference, improve the water turbulence and speed up the natural mixing in reservoirs. The sudden rise and fall of the water level may reduce the safety of dams. In 2016, the Oroville Dam suffered a sharp rise of water level due to the drastic climate change, leading to the damage of the main spillway. Therefore, it was necessary to study the impact of stress response to the operation and management of dams during the rainstorm.

To address the said problems, foreign scholars have conducted relevant researches on the daily change of water temperature in lake-type reservoirs, and found that solar radiation and wind force may affect the daily change of water temperature in reservoirs [10–13]. Zhu Bofang [14] concluded that annual changes in air temperature and water temperature would cause tensile stress in concrete dams, and corresponding measures should be taken; Wang Liangming [15] calculated the effects of daily temperature changes on the temperature field and temperature stress of concrete dams. Jia Chao [17] analyzed the interaction between water temperature and water pressure induced force through finite elements. The above literature all analyzed

This work is licensed under a CC BY-NC 4.0

the effects of temperature on the stress of concrete dams; however, few researches involved the dynamic change of temperature/stress of concrete dams under the combined effect of water level and water temperature during the heavy rain. Yigit [16] found that the periodic displacement response and linear displacement response of dams were related to seasonal temperature changes and linear rise of reservoir water level respectively, indicating that there was a correlation between temperature, water load and dam deformation. All of the said researchers have not studied the stress of dams under the combined action of temperature and water level. Based on these, this paper simulated a complete rainstorm by coupling water load and temperature load, and studied the changes of the dam stress during the rainstorm, which would provide a reference for the dam's safe operation during the heavy rain.

2. Methods

2.1. Prediction of reservoir water temperature under the storm flood

Research on the reservoir water temperature started in the 1950s. To date, the water temperature is mainly estimated through empirical methods, including Zhang Dafa method of the Northeast Survey and Design Institute [18] and Zhu Bofang method [19, 20] of China Institute of Water Resources and Hydropower Research which has been recorded into the Design Specification for Concrete Arch Dams [21]. Zhu Bofang's reservoir water temperature prediction model is as follows:

$$T_{sur} = T_{mod} + \Delta b \tag{1}$$

$$T_{mod} = \frac{1}{12}\Sigma_1^{12} T_i \tag{2}$$

where Δb means the temperature increment caused mainly by sunlight, °C; T_{mod} means the revised annual average temperature, °C. The initial water temperature at the bottom of the reservoir is selected based on the on-site measured data and corresponding empirical data.

After a reservoir is completed and begins to store water, under the impact of reservoir water level deepening and climate change, the water temperature layering will occur in the reservoir along the depth of water. The water temperature prediction is as shown above. The storm flood may disturb the initial water temperature, and the degree of disturbance can be determined by the runoff-reservoir capacity ratio method (i.e. parameter α-β method) according to the researches of Tao Mei et al. [22].

Typical parameters in the runoff-reservoir capacity ratio method (i.e. parameter α-β method) include:

$$\alpha = \frac{average\ annual\ runoff}{reservoir\ storage\ capacity} \tag{3}$$

$$\beta = \frac{\mathrm{Pr}imary\ flood\ capacity}{reservoir\ storage\ capacity} \tag{4}$$

Among the above parameters, when α < 10, the reservoir water temperature is in a stable layer; when α > 20, the reservoir water temperature is in a mixed layer; otherwise, it is in a transition layer. When the reservoir water temperature is in a stable layer, β > 1 indicates that the storm flood has an impact on the water temperature structure in the reservoir; β < 0.5 indicates that the storm flood has no effect on the water temperature structure in the reservoir; otherwise, the storm flood has a certain effect on the water temperature structure but doesn't damage the water temperature layering structure.

2.2. Calculation of rainfall-water level relationship

A heavy rain may finally turn into a flow in the reservoir area before the dam after runoff generation and concentration. With the rapid development of computers and continuous innovation of mathematical methods in recent years [23], rational formula method, empirical formula method, integrated unit hydrograph method and hydrological model method are often used to forecast the rainfall-flow relationship.

When calculating rainfall-runoff, the point rainfall is converted into the surface rainfall, and then the loss is subtracted to finally obtain the net rainfall. According to different conditions in different regions, the runoff generation is calculated using the principle of water balance, and then the rainfall is converted into runoff after the rain through the computing method of runoff concentration.

$$T_{sur} = T_{mod} + \Delta b \tag{1}$$

$$\begin{cases} Q_{mp} = 0.278(\frac{S_p}{\tau^n} - \mu)F & \tau = 0.278\frac{L}{ml^{1/2}Q_m^{1/4}} \quad (\tau_C \geq \tau) \\ Q_{mp} = 0.278(\frac{nS_p\tau_C^{1-n}}{\tau})F & \tau = 0.278\frac{L}{ml^{1/2}Q_m^{1/4}} \quad (\tau_C < \tau) \end{cases} \tag{5}$$

where Q_{mp} is the design flood peak flow, m^3/s; n is the rainstorm index, 0 < n < 1; S_p is the rain force, mm/h; τ_c is the duration of runoff generation, h; τ is the flow concentration time, h; F is the basin area, km^2; L is the flow length of the furthest point in the basin, km; m is the flow concentration parameter; I is the average vertical slope along the furthest flow; Q_m is the flood peak flow, m^3/s.

During a heavy rain, if the water level is lower than the crest level, the water level will gradually rise. The rising rate is positively correlated with the inflow quantity and the inflow duration. Generally, the reservoir capacity increment is the product of the inflow quantity and the inflow duration. The water level can be obtained from the capacity hydrograph at the dam site.

2.3. Computing theory of temperature field

The differential equation of heat conduction for a concrete structure is:

$$\frac{\partial T}{\partial t} = \alpha\nabla^2 T + \frac{\partial \theta}{\partial t} \tag{6}$$

where $\alpha = \frac{\lambda}{c_p\rho}$, ρ is the object density, kg/m^3. C_p is mass heat capacity at constant pressure, J/Kg*°C. λ is thermal conductivity, W/(m*°C). σ is the thermal diffusivity, m^2/s. $\nabla^2 = \frac{\partial^2}{\partial X^2} + \frac{\partial^2}{\partial Y^2} + \frac{\partial^2}{\partial Z^2}$, θ is the adiabatic temperature rise.

The corresponding initial conditions are:

$$T\big|_{t=0} = T_0(P), \left[P \in (v, s)\right] \tag{7}$$

Boundary conditions are:

$$T\big|s = T_b(P,t), \left(p \in s_1, t > t_0\right) \tag{8}$$

$$q_{n|s} = -\lambda\frac{\partial T}{\partial n}\bigg|_s = q_b(P,t), \left(P \in S_2, t > t_0\right) \tag{9}$$

where q represents the heat-flow density, $J/\left(m^2 * s\right)$, $P = P(x, y, z)$ represents the spatial point or spatial coordinate variable; N represents the direction of the outer normal. When $q_n = 0$ on a boundary surface, the boundary is an adiabatic boundary.

2.4. Finite element model

According to the engineering data and research needs, a typical project was selected for analysis. The dam is a C25 RCC gravity dam with the height of 61.6 m and the crest width of 6 m. Its downstream slope ratio is 1:0.75, the upstream slope ratio is 1:0.1, and the break point is 1/3 away from the dam heel. When established, the finite element model extended 40 m along the upstream, downstream and foundation respectively, and had a total of 17,400 nodes. In the calculation of the temperature field, the first boundary condition was taken on the contact surface between the dam body and the water, the second boundary condition was taken on the contact surface between the dam body and the air, and the adiabatic boundary condition was taken around the foundation; in stress calculation, normal constraints were imposed around the foundation, and full constraints were imposed at the bottom of the foundation.

2.5. Calculation parameters

Laboratory tests were performed according to the actual conditions of the project. The thermal parameters of the materials were shown in Table 1, and the mechanical parameters were shown in Table 2.

Table 1. List of thermal parameters of the materials.

material types	thermal conductivity (KJ/(m*h*°C))	thermal diffusivity (m2/h)	specific heat (KJ/(kg*°C))	linear expansion efficient (10^{-6}/°C)
foundation	9.8000	0.0034	1.0900	6.9200
C25 concrete	9.5800	0.0033	1.1000	6.8000

Table 2. List of mechanical parameters of the materials.

material types	elastic modulus （Gpa）	poisson ratio	axial compressive strength (N/mm^2)	axial tensile strength (N/mm^2)
foundation	22.00	0.20	10.00	1.27
C25 concrete	28.00	0.20	16.70	1.78

The temperature fitting formula is:

$$T_0 = \pi + R_0 t + A_0 \cos\left[\frac{\pi}{6}(t - 6.4)\right] \tag{10}$$

where T_0 is the average temperature, °C. A_0 is half of the difference between the maximum temperature and the minimum temperature; T is the time, month. $R_0 t$ is the ground temperature which can be ignored.

According to formulas (3) and (4), α was equal to 1.9 and β was equal to 1.2; therefore, the reservoir had water temperature layered. In case of a flood, the flood would make the water temperature structure mixed temporarily.

When there was no rain, the measured average annual water temperature on the surface was 13 °C and the water temperature at the bottom was 10.075 °C. The rainfall was mostly concentrated in July and August in the form of heavy rain, accounting for 54 % of the annual rainfall. The main stream of the reservoir contained 50 % sand. According to relevant researches [8, 9, 24, 25], the surface heat exchange did not directly act on the water layer below 15 m depth. During the flood season, the density currents fell to the bottom of the reservoir in the transition zone, and went ahead in the form of undercurrent until to the main reservoir area. The large inflow reduced the range of low-temperature water bodies and the depth of water temperature layer. Therefore, during calculation, it was considered that after storm water flowed into the reservoir, the water temperature before the reservoir was redistributed, and suddenly changed to 13 °C overall.

Due to the limited data, this paper was designed to quantitatively study the effect of the water level rising rate on the stress response of concrete dams when the water level rises from 58 m to 59.8 m under the same rainfall duration and the same amount of precipitation, and designed two working conditions: the first condition was the uniform rise of the reservoir water level at a rate of 0.0375 m/h, and the second condition was the S-shaped rise of the reservoir water level at a rate of 0.0425 m/h first and then at a rate of 0.0305 m/h.

3. Results and Discussion

3.1. Analysis of Calculation Results

3.1.1 Calculated result of temperature field

Through numerical simulation analysis, the results of the temperature field of the concrete dam were shown in Fig. 1.

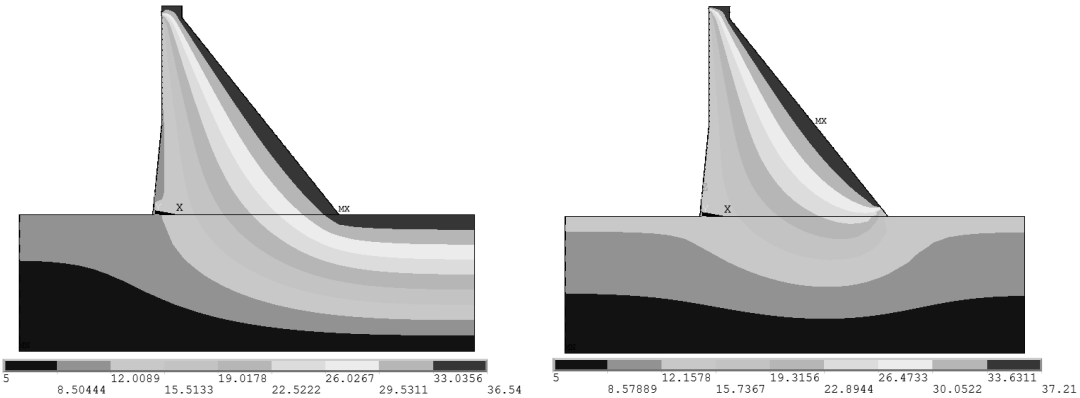

(a) Before the rain **(b) After the rain**

Figure 1. Distribution of dam temperature field (unit: °C).

It could be seen from the figure that under the dual effects of water temperature and air temperature, the dam body temperature changed. The dam foundation temperature was constant at 5°C. The temperature change on the surface of the dam body in contact with the air was consistent with the change of the local air temperature. Both changed in a trigonometric function and had no hysteresis.

3.1.2 Calculated result of stress field

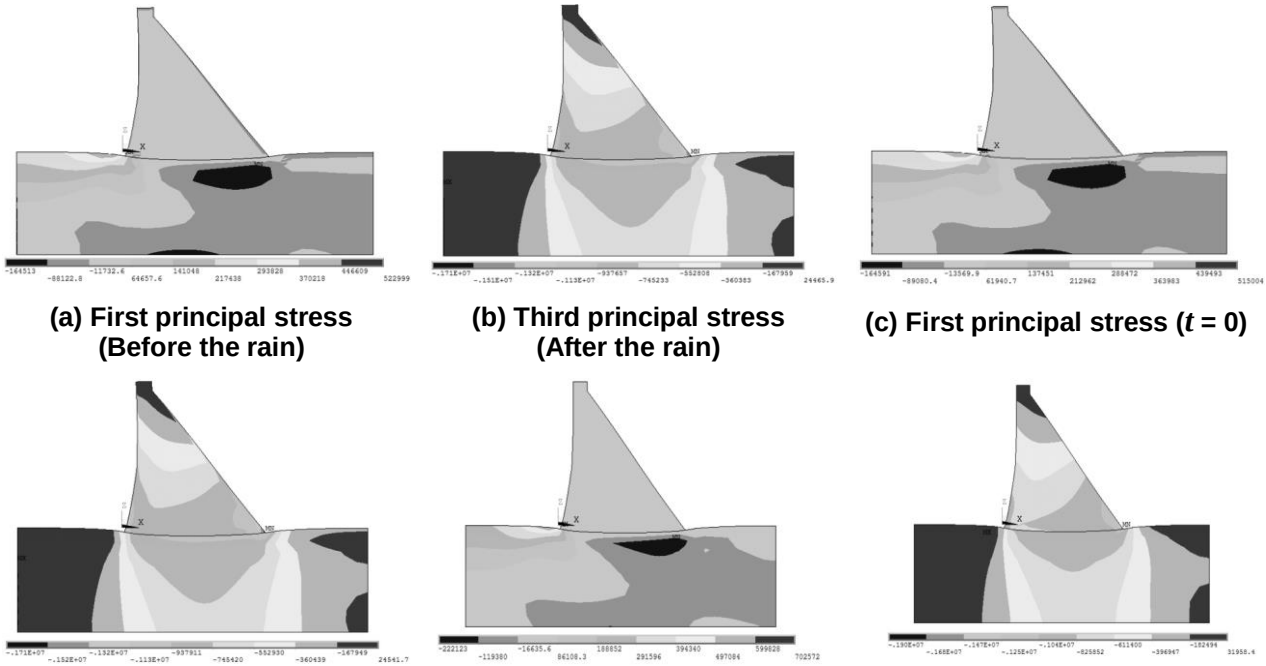

(a) First principal stress (Before the rain) **(b) Third principal stress (After the rain)** **(c) First principal stress (*t* = 0)**

(d) Third principal stress (*t* = 0) **(e) First principal stress (*t* = 24)** **(f) Third principal stress (*t* = 24)**

Figure 2. Distribution of stress field during uniform rise of reservoir water level (Unit: Mpa).

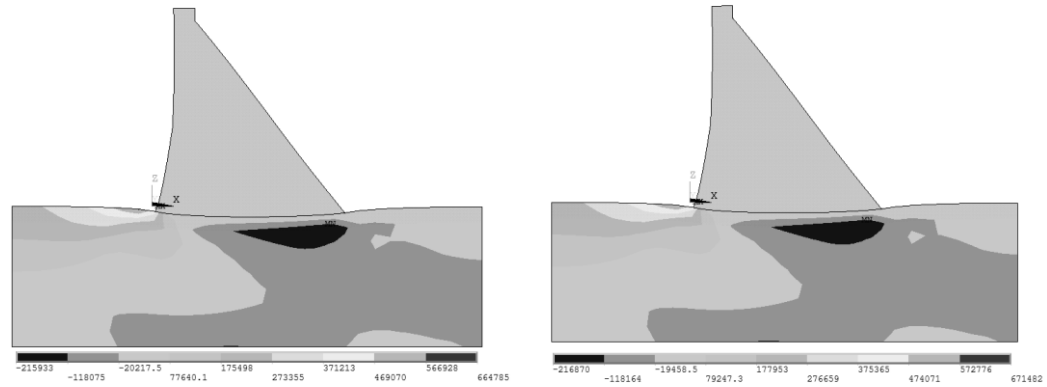

(a) Comparison of the first principal stresses

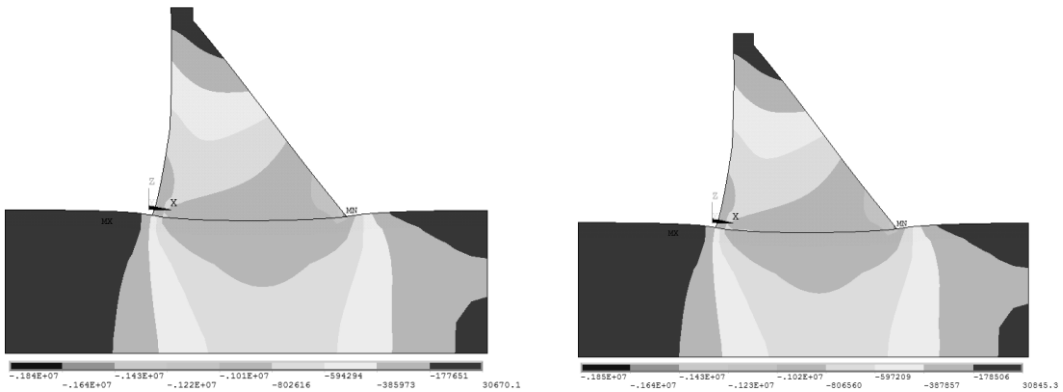

(b) Comparison of the third principal stresses

Figure 3. Comparison of stress fields under two working conditions (t = 14h, unit: Mpa).

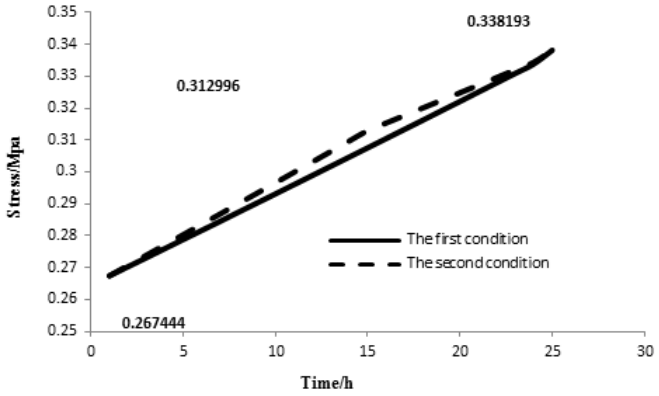

(a) Duration change of the first principal stress at the dam heel

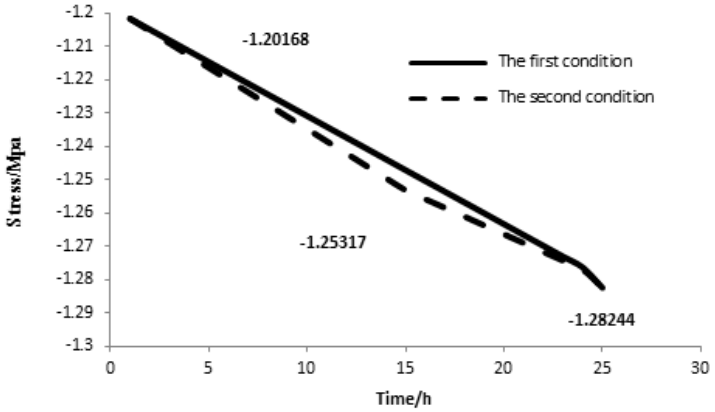

(b) Duration change of the third principal stress at the dam toe

Figure 4. Stress changes at feature points.

Table 3. Dam displacement table (unit: mm).

Time (h)	1	10	20	25
The first condition	1.01123	1.15733	1.31966	1.40091
The second condition	1.0116	1.17718	1.33519	1.42382

From the literature [16], the periodic displacement response and linear displacement response of dams were related to seasonal temperature changes and linear rise of reservoir water level respectively. A 58 m rise in the dam water level caused a dam displacement of 10 mm. As shown in Table 3, a 1.8 m rise in the water level caused a dam displacement of 0.4 mm. The dam displacement had a linear correlation with the rise of the water level. This result was consistent with the conclusions obtained by Yigit [16] through analysis of the measured data. This model was considered reasonable.

As we all know, the temperature stress is caused by the temperature difference. As shown in Fig. 2, before the storm flood flowed into the reservoir, the temperature was high at the dam crest and after the dam, and was low before the reservoir, the temperature difference, the temperature deformation and the temperature stress were all large; after the storm flood flowed into the reservoir, the water temperature in front of the reservoir was evenly distributed, the temperature difference between the upstream and downstream reduced, the temperature deformation of the dam body was small, and the temperature stress decreased. Therefore, the stress values in Fig. 2-(c) were greater than those in Fig. 2-(a). Since the temperature difference between the said stress values decreased 2.925 °C, the first principal stresses at the dam heel differed by about 2 KPa.

The water level rise after the storm flood entered the reservoir was shown in Fig. 2. As the flood continued to flow into the reservoir, the dam deformation increased, and the tensile stress and compressive stress were positively correlated with time. The maximum compressive stress occurred at the downstream dam toe, and lasted for two days with the value of 1.9 Mpa; the maximum tensile stress occurred at the upstream dam heel, and lasted for two days with the value of 0.7 Mpa, both of which did not exceed the allowable strength of concrete (allowable compressive stress: 16.7 Mpa, allowable tensile stress: 1.78 Mpa), and met the requirements for strength specified in the Design Specification for Concrete Gravity Dams.

As shown in Fig. 3, the stress of the dam body changed accordingly through comparison of two different reservoir water level rising rates. The faster the water level rose, the greater the response stress of the dam body was. When the water level rose for 14 h, the difference between the first principal stresses under the two working conditions was 0.0067 Mpa, and the difference between the third principal stresses was 0.01 Mpa. After the rainstorm entered the reservoir for 24 h, the water level and temperature became stable, so their stresses were the same.

4. Conclusion

To analyze the response of dams during the heavy rain, this study took a typical project in summer storm as an example, and adopted numerical simulations to analyze the changes of the temperature field and stress field of the dam body before and after the storm flood entered the reservoir. The results showed that:

1. Before and after the storm flood entered the reservoir, the temperature stress changed due to the change in the reservoir water temperature. For mixed reservoirs, the stress was reduced because the temperature difference between the upstream and downstream of the reservoir got smaller;

2. As the flood continued to enter the reservoir, the dam deformation increased, the changes in water temperature and air temperature had less effect, the water load had a significant effect, and the dam stress increased with the inflow of storm floods;

3. In the case of the same rainfall duration, the same rainfall amount, and the different rainstorm intensities, the water level rising rate had a significant effect on the stress response of the concrete dam body; that was, the faster the water level rose, the greater the dam stress was, which would damage the stability of the dam body and the bank slope in the reservoir area.

4. According to the literature [26], the heavy rain had a great impact on the stability of the bank slope in reservoir area; however, it needs further research in the later period.

Such results can provide a reference for the dispatching and operation of reservoirs in the rainy season, and can also provide a theoretical basis for the safe operation of cascade hydropower stations and the control of the water level rising rate.

5. Acknowledgements

This study was funded by the national key R & D plan fund project(2018yfc0406803) and Open project of dike safety and disease prevention engineering technology research center of the Ministry of water resources:(2018008)

References

1. Guoyu, R., Yu, C., Xukai, Z., Yaqing, Z., Xiaoling, W., Ying, J., Fumin, R., Qiang, Z. Definition and trend analysis of an integrated extreme climatic index (in Chinese). Climatic and Environmental Research. 2010. 15(4). Pp. 354–364..
2. Asadieh, B., Krakauer, N.Y., Fekete, B.M. Historical trends in mean and extreme runoff and streamflow based on observations and climate models. Water (Switzerland). 2016. 8(5). DOI: 10.3390/w8050189
3. Najibi, N., Devineni, N. Recent trends in the frequency and duration of global floods. Earth System Dynamics. 2018. 9(2). Pp. 757–783. DOI: 10.5194/esd-9-757-2018
4. Asadieh, B., Krakauer, N.Y. Global trends in extreme precipitation: Climate models versus observations. Hydrology and Earth System Sciences. 2015. 19(2). Pp. 877–891. DOI: 10.5194/hess-19-877-2015
5. Rifeng, L., Yang, L., Weixing, M., Zizhen, Z. Analysis of correlation between storm runoff and reservoir density current (in Chinese). 2017. Pp. 5−10. DOI:10.3969/j.issn.1673－9353.2017.05.006.
6. Ma, W., Huang, T., Li, X., Zhou, Z., Li, Y., Zeng, K. The effects of storm runoff on water quality and the coping strategy of a deep canyon-shaped source water reservoir in China. International Journal of Environmental Research and Public Health. 2015. 12(7). Pp. 7839–7855. DOI:10.3390/ijerph120707839.
7. Shiyong, H. Analysis of “99·7” storm flood and reservoir flood dispatching in Xin’an River Basin(in Chinese). HYDROLOGY. 2003. 23(1). Pp. 60–62.
8. Qike, X., Zhaowei, L., Yongcan, C., Xiao, C., Werk, K.T. Measurement and analysis of daily temperature changes in Xiluodu Reservoir(in Chinese). ADVANCES IN WATER SCIENCE. 2018. 29(4). Pp. 523–535. DOI:10.14042/j.cnki.32.1309.2018.04.008.
9. Kang, Z., Tinglin, H., Weixing, M., Zizhen, Z., Yang, L. Water-quality responses of the intrusion of high-turbidity runoff to the thermal stratified Jin-pen Reservoir during flood season (in Chinese). China Environmental Science. 2015. 35(9). Pp. 2778–2786.
10. van Emmerik, T.H.M., Rimmer, A., Lechinsky, Y., Wenker, K.J.R., Nussboim, S., van de Giesen, N.C. Measuring heat balance residual at lake surface using distributed temperature sensing. Limnology and Oceanography: Methods. 2013. 11(FEB). Pp. 79–90. DOI: 10.4319/lom.2013.11.79
11. Vercauteren, N., Huwald, H., Bou-Zeid, E., Selker, J.S., Lemmin, U., Parlange, M.B., Lunati, I. Evolution of superficial lake water temperature profile under diurnal radiative forcing. Water Resources Research. 2011. 47(9). Pp. 1–10. DOI: 10.1029/2011WR010529
12. Imberger, J. The diurnal mixed layer. Limnology and Oceanography. 1985. 30(4). Pp. 737–770. DOI: 10.4319/lo.1985.30.4.0737
13. MacIntyre, S., Romero, J.R., Kling, G.W. Spatial-temporal variability in surface layer deepening and lateral advection in an embayment of Lake Victoria, East Africa. Limnology and Oceanography. 2002. 47(3). Pp. 656–671. DOI: 10.4319/lo.2002.47.3.0656
14. Bofang, Z., Longshen, W., Yue, L., Guoxin, Z. Stress caused by annual temperature field changes during the gravity dam runtime (in Chinese). Water Resources and Hydropower Engineering. 2007. 38(9). Pp. 21–24. DOI:10.13928/j .cnki .wrahe.2007.09.002

15. He, W.S., Wang, L.M. Three-dimensional seepage field analysis of thick overburden CFRD after sealing failure. Applied Mechanics and Materials. 2014. 457–458. Pp. 797–800. DOI:10.4028/www.scientific.net/AMM.457-458.797.
16. Jia, C., Shao, A., Li, Y., Ren, Q. Analyses of thermal stress field of high concrete dams during the process of construction. Asia-Pacific Power and Energy Engineering Conference, APPEEC. 2010. (3). DOI:10.1109/APPEEC.2010.5449456.
17. Yigit, C.O., Alcay, S., Ceylan, A. Displacement response of a concrete arch dam to seasonal temperature fluctuations and reservoir level rise during the first filling period: evidence from geodetic data. Geomatics, Natural Hazards and Risk. 2016. 7(4). Pp. 1489–1505. DOI: 10.1080/19475705.2015.1047902
18. Dafa, Z. Analysis and estimation of reservoir water temperature(in Chinese). Journal of China Hydrology. 1984. 1. Pp. 19–27. DOI:10.19797/j.cnki.1000-0852.1984.01.006.
19. Bofang, Z. Prediction of water temperature in reservoirs (in Chinese). Journal of Hydraulic Engineering. 1985. 2. Pp. 12–21. DOI:10.13243/j.cnki.slxb.1985.02.002.
20. Ministry of Water Resources of the People's Republic of China. Design specification for concrete arch dams (in Chinese).
21. China, M. of W.R. of the P.R. of. Regulation for hydrologic computation of water resources and hydropower projects (in Chinese).
22. Mei, T., Yong, P., Hua, W., Kun, B. Effects of floods on reservoir temperature hierarchy(in Chinese). WATER RESOURCES PROTECTION. 2013. 29(5). Pp. 38–44.
23. Wang Fuqiang, H.F. Review on study of mid- and long-term hydrological forecasting technique(in Chinese). 2010. 27(5). Pp. 3–5. DOI: 10.3969/j.issn.1000-1379.2010.03.011
24. Wang, S., Qian, X., Wang, Q.H., Xiong, W. Modeling Turbidity Intrusion Processes in Flooding Season of a Canyon-Shaped Reservoir, South China. Procedia Environmental Sciences. 2012. 13(2011). Pp. 1327–1337. DOI: 10.1016/j.proenv.2012.01.125
25. Chung, S.W., Hipsey, M.R., Imberger, J. Modelling the propagation of turbid density inflows into a stratified lake: Daecheong Reservoir, Korea. Environmental Modelling and Software. 2009. 24(12). Pp. 1467–1482. DOI: 10.1016/j.envsoft.2009.05.016. URL: http://dx.doi.org/10.1016/j.envsoft.2009.05.016.
26. Siwei, W., Dezhi, J., Handong, L. Study of slope instability induced by rapid drawdown of water level (in Chinese). The first Geotechnical hydraulic Conference. 2005. Pp. 101–104.

Contacts:

Guo Lei, glboss@126.com
Shen Weiping, swpstudy@126.com
Guo Lixia, guolx@126.com
Wang Lunyan, 982069193@qq.com

© Lei, G.,Weiping, S.,Lixia, G.,Lunyan, W., 2020